A low power 8th order elliptic low-pass filter for a CMMB tuner

Gong Zheng(龚正)[1,†], Chen Bei(陈备)[1], Hu Xueqing(胡雪青)[1], Shi Yin(石寅)[1], and Dai Fa Foster(代伐)[2]

[1]Institute of Semiconductors, Chinese Academy of Sciences, Beijing 100083, China
[2]Department of Electrical and Computer Engineering, Auburn University, Auburn, AL 36849-5201, USA

Abstract: This paper presents an 8th order active-RC elliptic low-pass filter (LPF) for a direct conversion China Mobile Multimedia Broadcasting (CMMB) tuner with a 1 or 4 MHz –3 dB cutoff frequency ($f_{-3\mathrm{dB}}$). By using a novel gain-bandwidth-product (GBW) extension technique in designing the operational amplifiers (op-amps), the proposed filter achieves 71 dB stop-band rejection at 1.7 $f_{-3\mathrm{dB}}$ to meet the stringent CMMB adjacent channel rejection (ACR) specifications while dissipates only 2.8 mA/channel from a 3 V supply, its bias current can be further lowered to 2 mA/channel with only 0.5 dB peaking measured at the filter's pass-band edge. Elaborated common-mode (CM) control circuits are applied to the filter op-amp to increase its common-mode rejection ratio (CMRR) and effectively reject the large signal common-mode interference. Measurement results show that the filter has 128 dBμV$_{\mathrm{rms}}$ in-band IIP3 and more than 80 dB passband CMRR. Fabricated in a 0.35-μm SiGe BiCMOS process, the proposed filter occupies a 1.19 mm^2 die area.

Key words: CMMB tuner IC; continuous-time filter; active-RC filter; low power analog filter; gain-bandwidth-product extension; CMRR

DOI: 10.1088/1674-4926/32/9/095002 **EEACC:** 2570

1. Introduction

Nowadays, digital multimedia broadcasting systems for personal mobile terminals[1,2] are experiencing a rapid market growth with several standards such as DVB, DAB, T-DMB, ISDB-T and CMMB in each country, among which the CMMB announced in October 2006 provides audio, video and data services based on the Satellite and Terrestrial Interactive Multiservice Infrastructure (STiMi). CMMB uses S-band (2635–2660 MHz) for satellite, "gap-filler" for terrestrial broadcast and UHF band (470–862 MHz) for additional terrestrial broadcast. Its channel bandwidth can be either 2 or 8 MHz according to the data rate.

As a mobile TV standard similar to DVB-H, CMMB has stringent requirements on tuner power dissipation, sensitivity and selectivity. The $N-1/N+1$ digital and analog ACR specifications for CMMB standard are as high as 37 dB and 40 dB, respectively, which put great challenges on designing the channel select filters to achieve sharp transition-band, large stop-band attenuation and high linearity simultaneously. For this reason, active-RC topologies are often preferred to attain better linearity and dynamic range performances compared to their G_{m}–C counterparts due to the closed-loop configuration. However, active-RC type filters with sharp transition-band and large stop-band attenuation call for larger op-amp GBW[3] correspondingly. For a conventional two-stage Miller compensated op-amp, its GBW are approximately proportional to the bias current, leading to trade-offs between filter selectivity and power dissipation. To reduce the filter's bias current and make it suitable for mobile applications, several strategies could be adopted. In Ref. [4], extra feed-forward transconductor stages are used to increase the op-amps GBW. However, these extra stages introduce extra power dissipation and the local common-mode feedback scheme used in Ref. [4] may greatly reduce the op-amp output swings, leading to poor linearity. The conventional integrator frequency compensation scheme[5] by inserting resistors in series with the feedback integrator capacitors require the global zeros introduced by these resistors to track the op-amp GBW, which is hard to attain due to the intrinsic mismatch between the compensation resistor value and the op-amp input transconductance. Even with an automatic GBW tracking mechanism as in Ref. [6], high linearity of the filter is hard to reach in view of the relatively low op-amp GBW which has direct trade-offs with power dissipation.

In this paper, an 8th order elliptic filter of active-RC topology featuring 1 MHz or 4 MHz cut-off frequency is presented. By using a novel power-efficient op-amp GBW extension technique, the proposed filter achieves large stop-band attenuation, high linearity and low power dissipation simultaneously. The op-amps' common-mode behaviors are tightly controlled by applying a common-mode interference rejection (CMIR) circuit in addition to a common-mode feedback (CMFB) and a common-mode feed-forward (CMFF) circuit. Experimental results prove that the proposed skills are helpful in designing low power, highly linear channel select filters with large stop-band attenuation, high CMRR and good CMIR performances.

2. Filter architecture

The proposed 8th order elliptic LPF topology with 0.1 dB pass-band ripple as well as over 70 dB stop-band attenuation is synthesized based on the signal-flow graph (SGF) simulation method to derive low pass-band sensitivity from its LRC pro-

† Corresponding author. Email: rommel_gong@163.com
Received 19 March 2011, revised manuscript received 25 April 2011

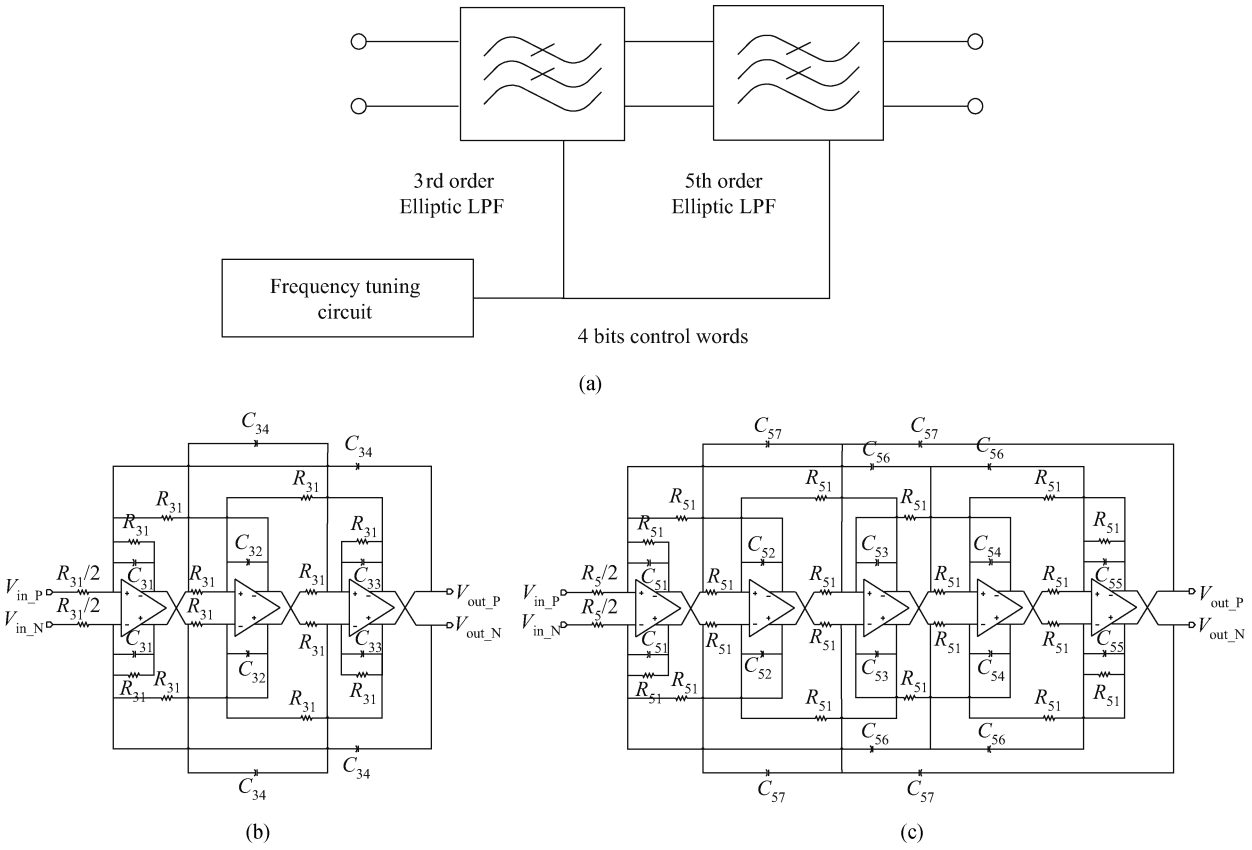

Fig. 1. (a) Overall filter architecture and the schematic of (b) the 3rd order and (c) the 5th order LPF.

totype. As shown in Fig. 1(a), the overall LPF comprises the 3rd order first filter (Fig. 1(b)) and the 5th order second filter (Fig. 1(c)) in cascading. Both filters share the same frequency tuning circuit, which automatically calibrates the RC time constant by a simple passive integrator based tuning circuit to derive the 4-bits control words of the filter's capacitor banks. As the first filter pre-attenuates the adjacent channel interference, the second filter can have less stringent linearity and selectivity specifications. In this way, the cascaded filter topology can lower the GBW requirements of the op-amps while achieving a sharp transition band and large stop-band attenuation. Moreover, the power dissipation of the two filters can be optimized separately by designing the op-amps with different GBW values.

3. Operational amplifier design

As described in Ref. [3], for a high Q filter of sharp transition-band and large stop-band attenuation, its Q deviation from the RLC prototype has the following relationship with the op-amp GBW:

$$\Delta Q \approx \frac{2\omega_c Q}{\mathrm{GBW}}, \tag{1}$$

where Q, ΔQ and ω_c stand for the quality factor, Q deviation and cut-off frequency of the filter prototype, respectively. Equation (1) shows that extending the op-amp GBW can effectively lower the Q deviation and thus the magnitude peaking at filter pass-band edge and prevent the filter from oscillation. In this design, an op-amp GBW extension scheme without extra power dissipation based on the idea of "anti-pole splitting" is presented. In the rest of this section, Section 3.1 discusses this method in detail and Section 3.2 describes the op-amp common-mode control circuits.

3.1. Gain-bandwidth product extension

Figure 2(a) shows the simplified schematic of the op-amps used in the proposed LPF. It is a two-stage op-amp. The signal path consists of a PMOS input stage and an output stage built with NPN transistors to improve the transconductance efficiency. The common-mode control section includes the CMIR, CMFF and CMFB circuits as shown. A novel GBW extension structure splits the conventional Miller compensation capacitor C_c into two identical ones C_{C1}, C_{C2} in series, each with two times the C_c value to achieve the same pole-splitting effect as in conventional two-stage Miller op-amps. R_Z is used to cancel out the right half plane (RHP) zero and R_1 acts as an "anti-pole splitting" resistor[7] at low frequencies, by which the op-amp GBW can be greatly increased without consuming extra current. R_2 operates on common-mode signals only to cancel out the "anti-pole splitting" effect for the op-amp common-mode loop, which will be discussed later in part B.

The op-amp differential mode small signal equivalent circuit is shown in Fig. 2(b). The proposed GBW extension principle can be explained as follows:

At low frequencies, R_1 has lower impedance than C_{C1} and the feedback current signal flows through C_{C2}, R_1 to AC ground. Since only small part of the feedback current flows

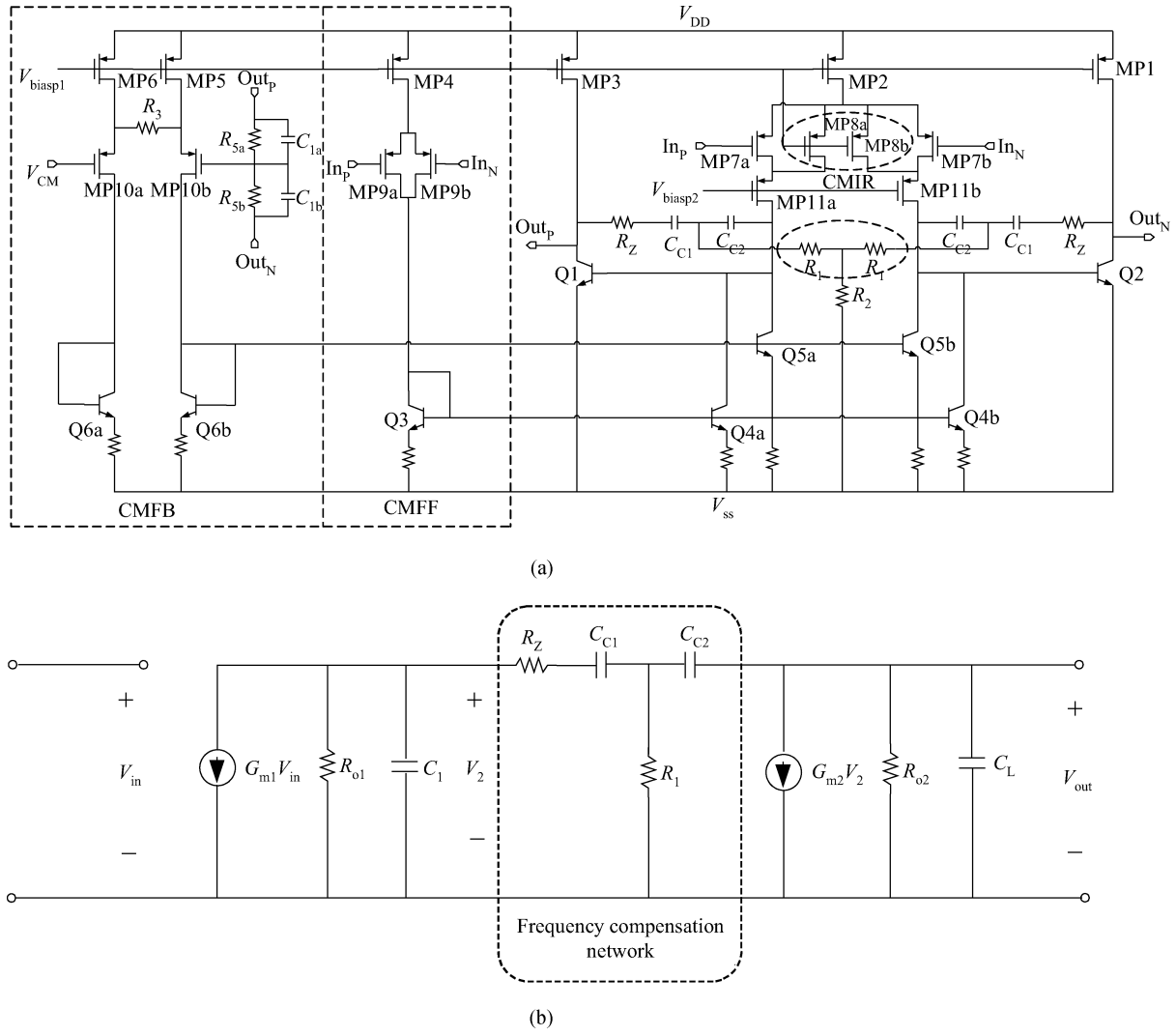

Fig. 2. (a) The simplified schematic of the proposed GBW extended op-amp and (b) its differential mode small signal equivalent circuit.

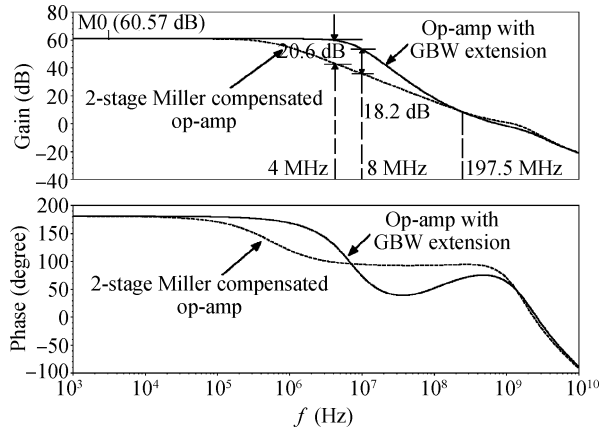

Fig. 3. AC response of the proposed GBW extended op-amp in comparison with that of a conventional Miller compensated op-amp.

through C_{C1}, the feedback path is now cut off, presenting the effect of "anti-pole splitting". As a result, the op-amp behaves like an uncompensated two stage amplifier with the AC magnitude response exhibiting a two-pole roll-off with a –12 dB/oct. rate, and the roll-off corner frequency is higher comparing to the conventional Miller compensated op-amp. At high frequencies, C_{C1} has lower impedance than R_1 and steers the feedback current as in the conventional Miller compensated op-amps, making its magnitude response coincides with the Miller compensation response with a single-pole roll-off rate of –6 dB/oct.

As depicted in Fig. 3, the two frequency response curves of a conventional Miller op-amp and the proposed op-amp with extended GBW intersect at a frequency around $1/2\pi R_1 C_{C1}$, which is 197.5 MHz in this design. As shown in this figure, the proposed GBW extension scheme can substantially increase the Op-Amp gain by more than 20 dB at the filter's f_{-3dB} of 4 MHz, and by 18.2 dB at $2f_{-3dB}$ of 8 MHz, while dissipating the same bias current. Both in-band and out-of-band linearity can be significantly enhanced attributing to this open loop gain improvement. Moreover, pass-band ripple of the filter response can be reduced with lower op-amp power dissipation compared to the conventional Miller structure.

By using the proposed GBW extension technique, the op-amp phase margin decreases only by 2° compared to its Miller compensated counterpart, with the simulation results larger than 55° over process, voltage and temperature (PVT) vari-

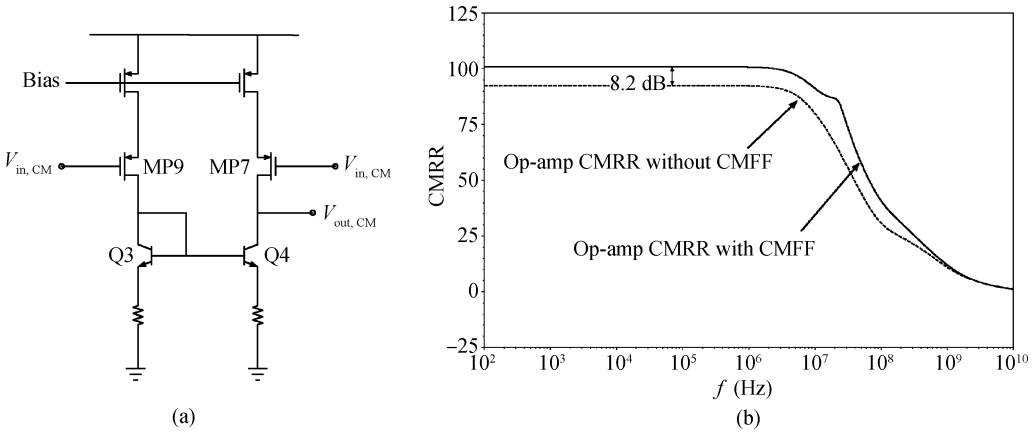

Fig. 4. CM equivalent circuit of (a) the op-amp 1st stage and (b) simulated CMRR.

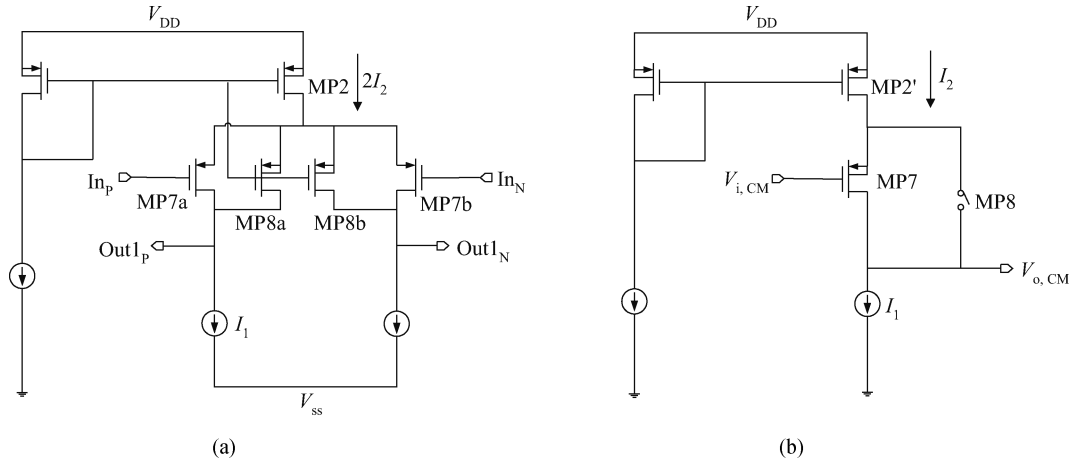

Fig. 5. (a) Simplified schematic of the op-amp's 1st stage and (b) its CM equivalent circuit.

ations. The non-monotonic phase response of this structure would not endanger the filter's stability by careful design as explained in Ref. [8], which is also verified in this design by the extensive transient simulations and experimental results. The only prices paid for using this method are a little more die area occupied by adding resistors R_1, R_2 and four times die area of the original compensation capacitors, which is often negligible for high GBW op-amp design due to their small absolute values.

3.2. Common-mode control circuits

To improve the filter's linearity and common mode stability, the CM behavior of the op-amps should be tightly controlled.

In Fig. 2(a), the common-mode feedback amplifier stabilizes the op-amp common-mode output voltages. R_2 used for canceling out the "anti-pole splitting" effect of the CM loop is designed to be tens of kilo ohms to ensure that the CM loop response of the proposed op-amp is similar to that of its Miller compensated counterpart.

As discussed in Ref. [5], building up op-amps with intrinsic high CM rejection not only helps to improve the filter's CMRR performance, but also makes the CM loops across the integrators of high order active filters more stable. In this design, op-amp CMRR is improved by adding an auxiliary input CM transconductor made up of MP9a, MP9b and current mirror Q3, Q4 in parallel with the op-amp input stage comprising MP7a, MP7b, and Q5 (Fig. 4(a)). As demonstrated in Fig. 4(b), a CMFF path formed by this auxiliary transconductor can provide 8.2 dB CMRR bonus at the expense of only 10 μA extra bias current for each op-amp.

Moreover, to reject the large signal CM interference, two PMOS transistors MP8a, MP8b are added to the op-amp's input stage as shown in Fig. 5(a). Their gate–source voltages are identical to that the tail current device MP2, and the threshold voltages V_{thp} of MP2, MP8a and MP8b can also be regarded as equal by connecting the PMOS bodies to their drains to eliminate the body effect.

When there is no CM interference applied to the input terminals In_P and In_N, the input pair MP7a, MP7b and the tail current source MP2 are biased in saturation region with $\left|V_{gd, MP2}\right| < V_{thp}$. MP8b, MP8b are now turned off and dissipates no quiescent current. When the op-amp inputs catch a large CM step, MP8a, MP8b function as switches as demonstrated in Fig. 5(b). Without these two devices, the large CM step would turn off the input devices MP7a and MP7b, starve the PMOS tail current I_2 and drastically pull the op-amp output CM voltage away from its nominal CM value to the power rail. The near to rail output CM voltage may continue to saturate the

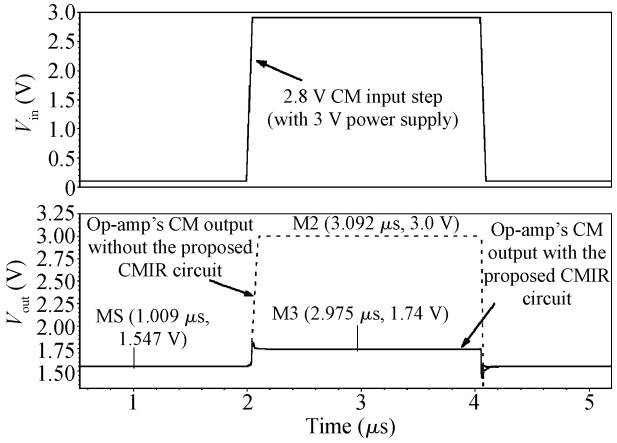

Fig. 6. Op-amp's CM response to a 2.8 $V_{p\text{-}p}$ step.

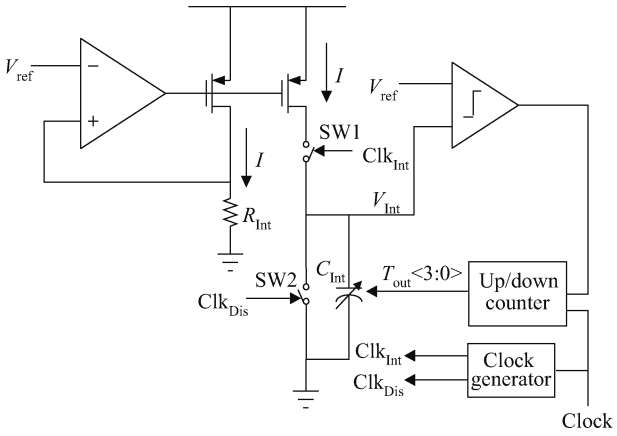

Fig. 7. Automatic frequency tuning circuit.

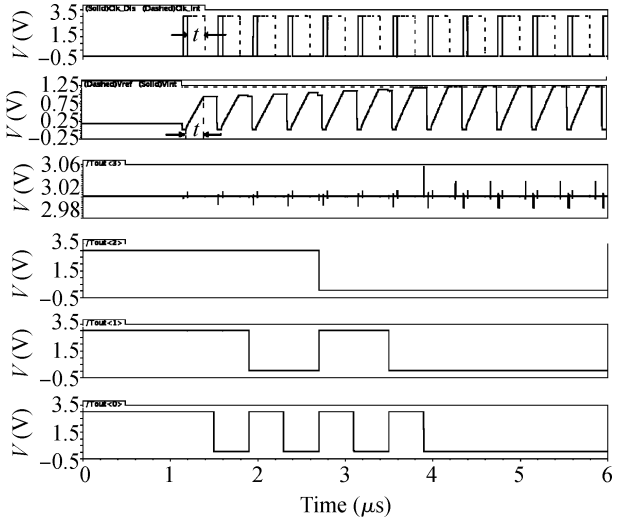

Fig. 8. Switch-timing diagram of the automatic tuning system.

following op-amps and finally put the filter into latch or CM oscillation status. When MP8a and MP8b are added, the large CM step would firstly push up the source voltages of the input pair and drive MP2 to triode region with $\left|V_{\mathrm{gd,MP2}}\right| > V_{\mathrm{thp}}$. This will turn on MP8a and MP8b soon, conduct I_2 to the output to balance the upper and lower bias currents and maintain

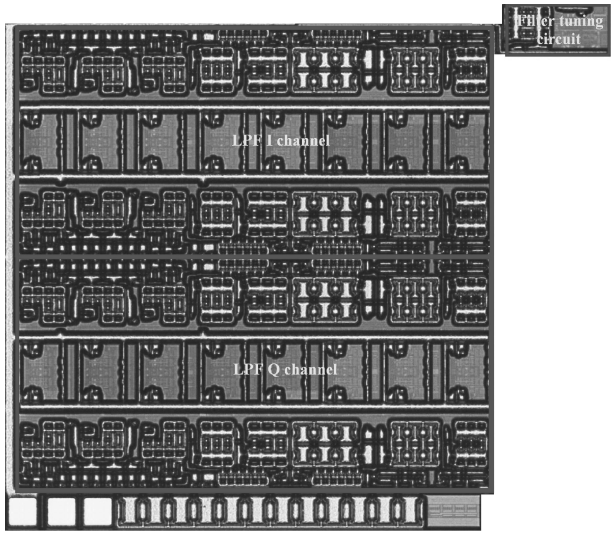

Fig. 9. Filter die photograph.

the output CM voltage around its nominal CM value. As shown in Fig. 6, by applying such two simple devices, the op-amp's output CM spike in response to a 2.8 $V_{p\text{-}p}$ CM step under 3 V supply reduces from half of the power supply voltage to only 193 mV, which is small enough to prevent the following op-amps from latching. The attenuated CM interferes can now be regarded as small signal CM noise, and further rejected by following op-amps.

4. Automatic frequency tuning circuit

An automatic frequency tuning circuit is often required by continuous-time active-RC filters to calibrate the RC constant to account for over +/–20% PVT variations of RC product. Figure 7 shows the simple automatic frequency tuning circuit used in this design[1]. Its switch-timing diagram is shown in Fig. 8.

In Fig. 7, R_{Int} and C_{Int} of the passive integrator are implemented with the same kind of resistors and capacitors as used in the active-RC integrators, respectively. The clock generator produces two clock signals: $\mathrm{Clk_{Dis}}$ for discharging the capacitor bank C_{Int} while $\mathrm{Clk_{Int}}$ for charging it. By periodically comparing the voltage across C_{Int} after each charging process with V_{ref} and successively tuning the 4-bit capacitor bank control word, V_{int} is finally charged approximately equal to V_{ref} and the RC constant is determined only by the reference clock frequency as:

$$V_{\mathrm{Int}} = \frac{Q}{C} = \frac{t(V_{\mathrm{ref}}/R_{\mathrm{Int}})}{C} \approx V_{\mathrm{ref}}, \tag{2}$$

$$R_{\mathrm{Int}}C_{\mathrm{Int}} = t = K/f_{\mathrm{clock}}, \tag{3}$$

where K is a given constant, f_{clock} and t stands for the clock frequency and the charging period time, respectively.

5. Experimental results

The 8th order low-pass filter is fabricated in a 0.35-μm SiGe BiCMOS process. Its die photograph is shown in Fig. 9,

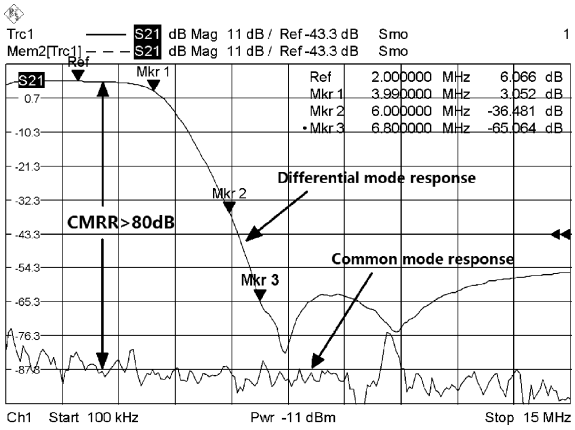

Fig. 10. Differential mode and common-mode frequency responses.

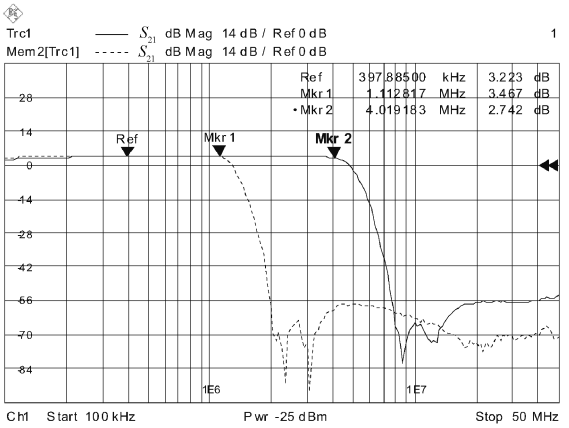

(a)

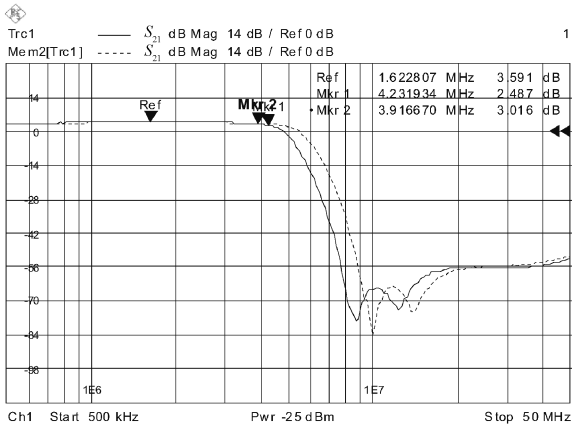

(b)

Fig. 11. (a) Filter bandwidth switching (4 MHz—Solid, 1 MHz—Dashed) and (b) its frequency responses with (solid) and without (dashed) automatic tuning.

in which the active area of the filter I/Q channel and the automatic frequency tuning circuit are $1120 \times 1050\ \mu m^2$ and $240 \times 110\ \mu m^2$, respectively. An off-chip buffer with 4 dB gain is used in the test. The filter chip excluding the test buffer consumes 5.8 mA from a 3 V supply.

The measured differential mode and common-mode frequency responses are shown in Fig. 10 with the filter's cut-off frequency set to 4 MHz, where the stop-band attenuation at $2f_{-3dB}$ is as large as 71 dB and the measured filter CMRR in the passband is higher than 80 dB. The CM gain of less than –75 dB is achieved even in the stopband. Figure 11(a) demonstrates that the filter's cut-off frequency can be switched between 4 MHz and 1 MHz to fulfill the CMMB channel select requirements and Figure 11(b) shows the filter's frequency response before and after automatic frequency tuning with 4 MHz bandwidth. Based on the lab results, less than +/−3% cut-off error is achieved.

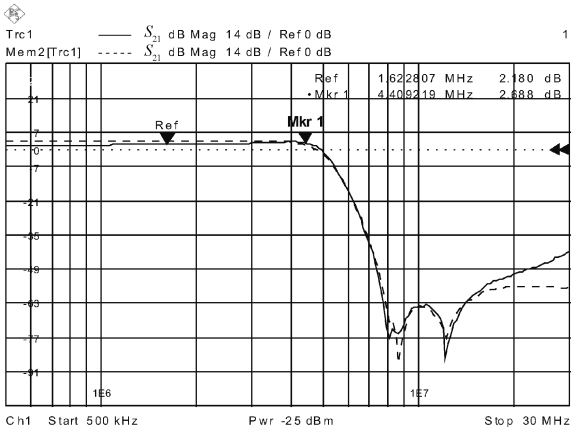

Fig. 12. Comparison of filter frequency responses with 2.8 mA/channel (dashed) and 2 mA/channel (solid) bias current.

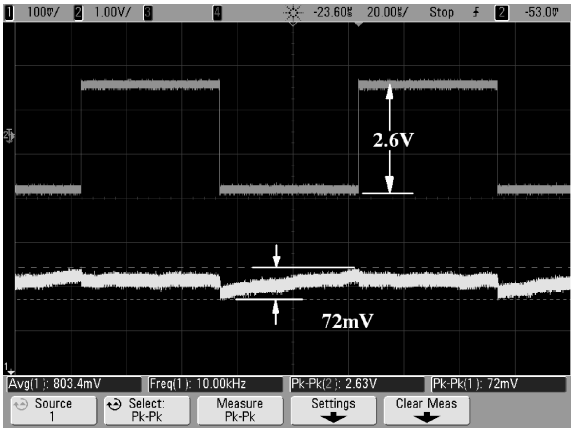

Fig. 13. Op-amp common-mode transient response.

The bias current of the proposed filter op-amps are designed to be tunable by an off-chip resistor to explore the relationship between filter power dissipation, its op-amp GBW and the magnitude peaking in frequency responses. In Fig. 12, the filter bias current is lowered from its nominal value of 2.8 mA/channel to 2 mA/channel, resulting in only 0.5 dB magnitude peaking detected at the passband edge.

Figure 13 plots the filter's CM response to a 2.6 $V_{p\text{-}p}$ CM input step under 3 V power supply. It can be found that by applying the proposed CMIR to the op-amp input stages, the filter's output CM spike is as small as 72 mV, notwithstanding the near rail-to-rail input CM interference.

Linearity performances are measured by applying two input tones at 1 MHz and 1.2 MHz to the filter which is configured at 4 MHz cutoff frequency with 2.1 dB passband gain. Figure 14 shows the measured results. The measured IM3 at 1.4 MHz output is 72 dB with 90 dBμV_{rms} input and the cal-

Table 1. Summarized filter experimental results in comparison with the referenced works.

Parameter	Ref. [2]	Ref. [9]	This work
Technology	0.25 μm BiCMOS	0.35 μm CMOS	0.35 μm BiCMOS
Filter order	5th order elliptic	5th order Butterworth	8th order elliptic
Area (mm^2/channel)	0.68	4.8	1.19
Supply (V)	2.4-3	2.7-3	3
I/pole (mA)	0.5	0.94	0.36
Cutoff frequency (MHz)	4	2.1	4
Stop-band attenuation (dB)	60 @ $2f_{-3\mathrm{dB}}$	30 @ $2f_{-3\mathrm{dB}}$	42 @ $1.5f_{-3\mathrm{dB}}$, 71 @ $1.7f_{-3\mathrm{dB}}$
CMRR (dB)	N/A	N/A	> 80
IIP3 (dBμV$_{\mathrm{rms}}$)	128	155	128
Noise density (nV/$\sqrt{\mathrm{Hz}}$)	45.3	32.4	31

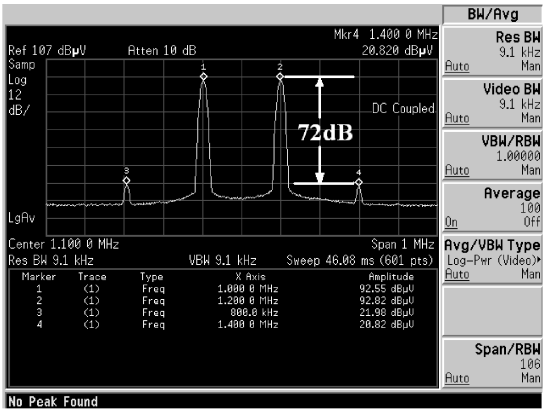

(a)

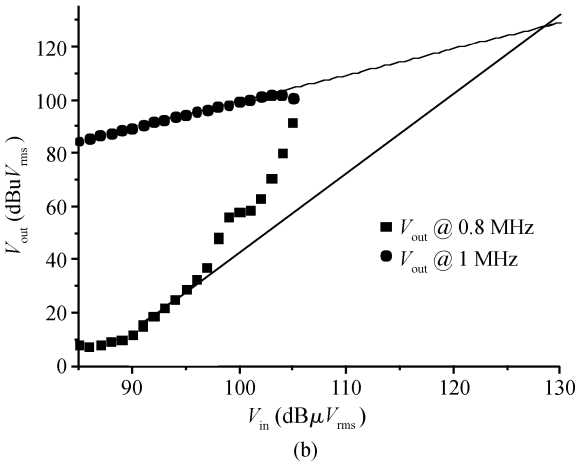

(b)

Fig. 14. (a) Measured IM3 with 90 dBμV_{rms} input 2-tones and (b) the measured in-band IIP3.

culated filter in-band IIP3 is about 128 dBμV$_{\mathrm{rms}}$. The performance characteristics of the proposed LPF are summarized in Table 1 with comparison to the referenced works. It can be concluded that the proposed LPF achieves comparable noise and linearity performances but has significantly larger stop-band attenuation and dissipates less power compared to its BiCMOS and CMOS referenced counterparts, which fulfills the CMMB mobile application.

6. Conclusion

An 8th order active-RC elliptic LPF for CMMB tuner IC application is implemented with a 0.35-μm SiGe BiCMOS process. By utilizing op-amps with a novel power-and-area-efficient GBW extension technique, the proposed LPF achieves low power, high linearity and large stop-band attenuation simultaneously and effectively reduces the magnitude peaking at the filter's pass-band edge. Tight CM control is applied to the op-amps to get large CMRR performances and effectively reject the large signal CM interferences to prevent the filter forming CM oscillation and latch status. The proposed techniques are general and as such can be applied to any low power, low voltage channel select filter design.

Acknowledgments

The author would like to thank He Juan, Zhou Changlei, Wu Zhaosheng and Guan Xin for their help in layout and testing.

References

[1] Kim S, Kim B, Jeong M S, et al. A 43 dB ACR low-pass filter with automatic tuning for low-IF conversion DAB/T-DMB tuner IC. Proc Eur Solid State Circuits Conf (ESSCIRC), 2005: 319

[2] Notten M, Brekelmans H, Rambeau V. A 5th order 14 mWatt active polyphase filter for analog and digital TV on mobile applications. Proc Eur Solid State Circuits Conf (ESSCIRC), 2006: 211

[3] Kousai S, Hamada M, Ito R, et al. A 19.7 MHz, fifth-order active-RC Chebyshev LPF for draft IEEE802.11n with automatic quality-factor tuning scheme. IEEE J Solid-State Circuits, 2007, 42(11): 2326

[4] Harrison J, Weste N. A 500 MHz CMOS anti-alias filter using feed-forward op-amps with local common-mode feedback. IEEE Int Solid-State Circuit Conf Dig Tech Papers, 2003: 132

[5] Tsividis Y P. Integrated continuous-time filter design—an overview. IEEE J Solid-State Circuits, 1994, 29: 166

[6] Wan P, Chiu Y, Lin P. A 5.8-mW, 20-MHz, 4th-order programmable elliptic filter achieving over –800 dB IM3. Proc CICC, 2010: 1

[7] Fast Compensation Extends Power Bandwidth, National Semiconductor Linear Brief 4, Apr 1969

[8] Vasilopoulos A, Vitzilaios G, Papananos Y. A low-power wideband reconfigurable integrated active-RC filter with 73 dB SFDR. IEEE J Solid-State Circuits, 2006, 41(9): 1997

[9] Hollman T, Lindfors S, Lansirinne M, et al. A 2.7-V CMOS dual-mode baseband filter for PDC and WCDMA. IEEE J Solid-State Circuits, 2001, 36: 1148